Code-adaptive Transmission Accounting for Filtering Effects in EON

Gianluca Meloni, and Luca Potì
Photonics Networks National Laboratory, CNIT,
Pisa, Italy
Email: gianluca.meloni@cnit.it

Nicola Sambo and Francesco Fresi
TECIP, Scuola Superiore Sant'Anna,
Pisa, Italy

Fabio Cavaliere
Ericsson Research,
Pisa, Italy

***Abstract*—Terabit/s Time-Frequency-Packing (TFP) super-channel transmission based on code-adaptation is demonstrated for elastic optical networks. Code is set to achieve error free transmission accounting for physical layer impairments including filtering effects. High spectral-efficient transmission (e.g., 6.6 b/s/Hz with low-order format polarization multiplexing quadrature phase shift keying —PM-QPSK) is achieved in an elastic optical network (EON) experimental testbed including fiber transmission and filters. Monitoring of the super-channel is also enabled to reveal possible signal degradations. In case, hitless code adaption is performed to re-act to the degradation without the need of any re-routing.**

I. Introduction

The continuous increase of bandwidth request and traffic dynamicity is paving the way to EONs, where optical circuits (lightpaths) are switched in portions of spectrum whose width depends on the supported bit rate and transmission technique (e.g., modulation format) [1]–[4]. Thus, in order to efficiently use the optical spectrum, spectral efficient transmissions are investigated, such as high-order modulation formats [5]–[7] or faster-than-Nyquist transmission as *time frequency packing (TFP)* [8]–[10]. Differently from Nyquist transmission, TFP consists in sending pulses that strongly overlap in frequency or time, thus achieving high spectral efficiency, but introducing inter-symbol interference (ISI). Low density parity check (LDPC) code and coherent receiver are properly designed to account for signal degradations including ISI [9]. TFP achieves distance adaptation through coding, and transponders may just support only a single modulation format, such as PM-QPSK. In particular, the amount of code redundancy can be tuned based on the physical characteristics of the path, e.g. more redundancy would be need for more impaired paths. Because of the introduced ISI, TFP also requires sequence detector instead of symbol-by-symbol detector. On the other hand, by using only PM-QPSK, digital-to-analog converter can be avoided. TFP aims at providing robust transmission guaranteeing high spectral efficiency.

Although nowadays spectral efficient transmission techniques have been proposed and demonstrated, EONs still present some issues that may limit such efficiency. More specifically, switching in EONs is based on reconfigurable filters: spectrum selective switches (SSSs). Currently, such filters do not present an ideal rectangular shape and their non-negligible transition bands may introduce distortions on the signal [9], [11]. In order to limit these effects, larger filters' passband should be configured, thus increasing the occupied spectrum resources and limiting the spectral efficiency. Regarding TFP, filtering effects on such transmission technique require to be more deeply investigated.

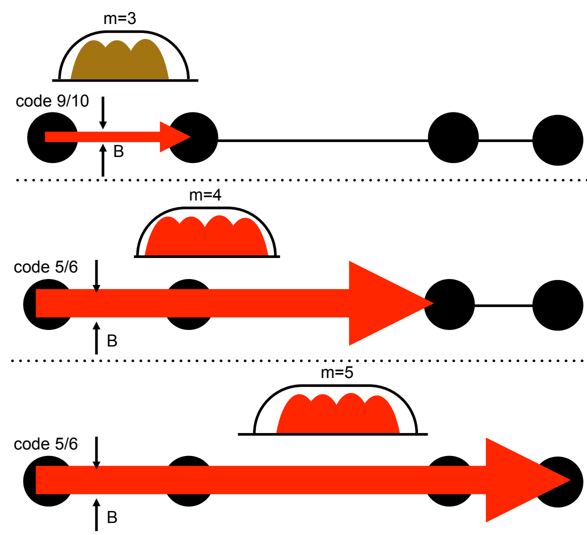

Fig. 1. Example of super-channel configuration.

In this paper, we demonstrate error-free 1 Tb/s code-adaptive transmission in the presence of physical layer degradations, including filtering effects. Code rate is selected based on the required optical reach and on the number of nodes to be traversed. Filter passband is decided according to the selected code and filtering effects guaranteeing error free transmission. Measurements in the EON testbed show that TFP with the jointly selection of code and filter passband guarantee paths with several hops and very high spectral efficiency, e.g. 6.6 b/s/Hz with PM-QPSK. We also demonstrate hitless code adaptation on a working lightpath upon signal degradation: the degradation is introduced on an active super-channel, then a monitoring system produces an alarm and code is dynamically adapted/changed to avoid performance degradation. Such operation is demonstrated in an hitless way without the need of re-routing the super-channel.

978-3-9018-8272-2/15 ©2015 IFIP

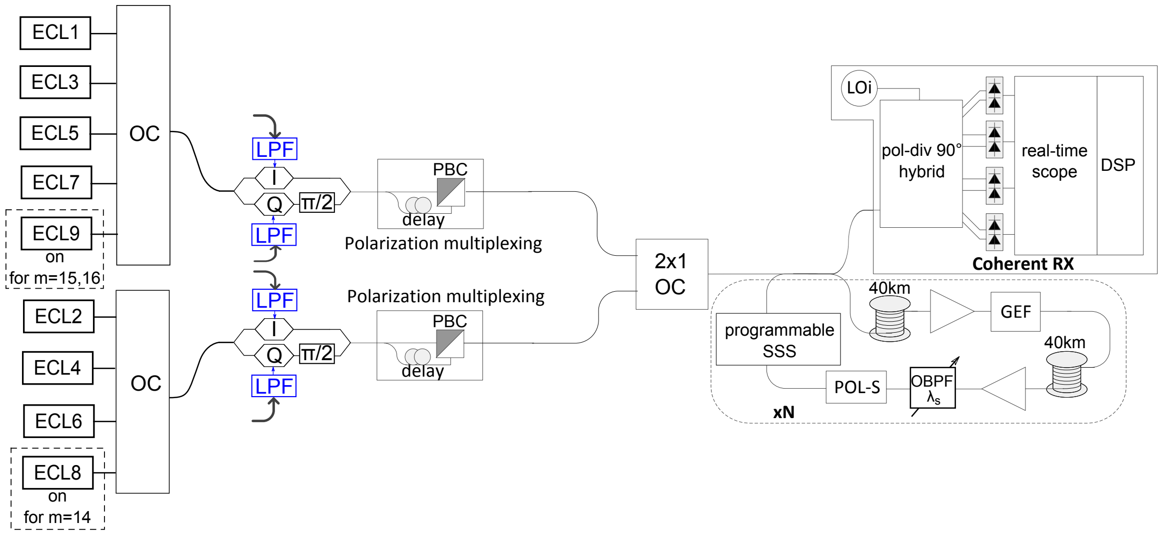

Fig. 2. Experimental testbed.

II. Setting code, sub-carriers, and filters, and code adaptation

A transponder supporting TFP is assumed. A super channel at (gross) line rate R is obtained by transmitting N PM-QPSK optical sub-carriers. The line rate of each sub-carrier is R_s and the overall super-channel bandwidth is B. R is given by $N \times R_s$. TFP is exploited to reduce the bandwidth B_s of each sub-carrier and their frequency separation S below the Nyquist limit. LDPC code is used to approach the maximum information rate achievable with the given modulation, accounting for the presence of noise, fiber non-linear effects, filtering, and ISI. R includes the information rate R_I and the code rate R_C, in particular $R_I = R \times R_C = N \times R_s \times R_C$. R_C is defined as i/b, meaning that $(b-i)$ bits of code are placed each i bits of information. The receiver of each sub-carrier exploits coherent detection with digital signal processing (DSP) and decoding. In particular, a two dimensional adaptive feed forward equalizer recovers the four signal quadratures, compensating for linear propagation impairments (e.g., group-velocity dispersion and polarization-mode dispersion) and completing the implementation of the matched filter required for detection. Then, a maximum a posteriori symbol detector, which takes the form of the Bahl-Cocke-Jelinek-Raviv (BCJR) detector [12], iteratively exchanges information with an LDPC decoder according to the turbo principle [13].

To address EON requirements, code rate can be set to provide adequate robustness to the transmission. An example is shown in Fig. 1 where we assumed a fixed information rate R_I and a given $B_s = S$. The example shows that $R_C = 9/10$ guarantees acceptable quality of transmission (QoT) for the single-hop path assuming an ITU-T *frequency slot* width of m=3 [14][1]. However, to traverse one hop more, higher redundancy has to be exploited and $R_C = 5/6$. The increase of redundancy may result in the increase of N to guarantee the fixed information rate, given $R_I = N \times R_s \times R_C$. Thus, in the example another sub-carrier is added to the super-channel in order to satisfy the requested R_I. The increase of N also implies the increase of m, thus the bandwidth to be switched. Finally, the example shows that, to traverse the three-hop path, the same R_C can be kept (thus, a further sub-carrier is not involved), but filters must be enlarged (m=5) to avoid excessive degradations due to filtering. In the next section, we will show an empiric relation between the code, the number of traversable hops, the number of sub-carriers, and the ITU-T frequency slot width.

Once the connection is established according to the computed transmission parameters, code can be changed, dynamically addressing either degradation of transmission performance or optimization of configured resources (e.g., avoiding the use of excessively redundant coding which would provide unnecessary additional robustness at the expenses of a larger amount of occupied spectrum resources). If adaptation implies a change of the number of active sub-carriers or of the reserved spectrum resources, the control plane has to be typically involved (e.g., through an active Path Computation Element as in the case of [15]). On the other hand, as shown in the next section, adaptation can be applied on coding with no control plane operations when N or the bandwidth do not change.

Monitoring functionalities in the digital signal processing (DSP) at the receiver are exploited. In particular, the variance of the received symbols can be monitored to detect a signal degradation before experiencing performance degradation, thus before experiencing an increase of the bit error rate. A variance increase may be due to OSNR degradation. Once a suspect variance increase is detected, an hitless dynamic code adaptation through the change of R_C can be performed via software. The technique will be successfully demonstrated in the next section to increase transmission robustness, such

[1]According to the ITU-T flexible grid, connections can be switched in *frequency slots*, i.e. portions of bandwidth defined as $m \times 12.5$ GHz, with m an integer

978-3-9018-8272-2/15 ©2015 IFIP

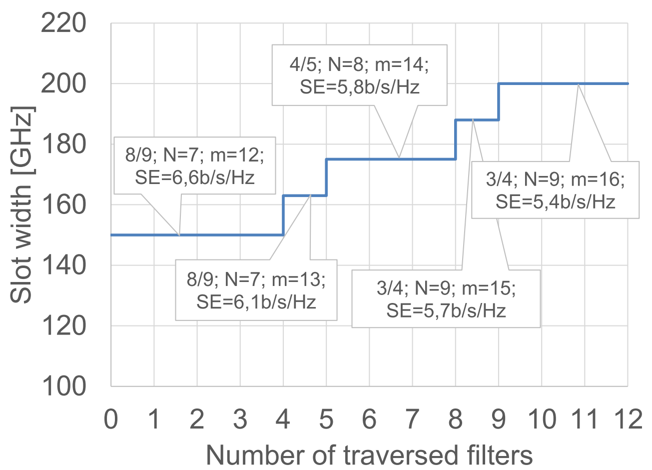

Fig. 3. Slot width for super-channel at varying the number of traversed loops.

that no traffic disruption is experienced and no-rerouting is performed.

III. Measurements

A. Experimental set-up

The experimental testbed is depicted in Fig. 2. N optical carriers are generated by means of 100 kHz linewidth tunable laser sources (TLSs). The odd an even channels are modulated separately by means of two integrated double nested Mach Zehnder modulators (IQ-MZM). 40 Gb/s LDPC-coded electrical signals are applied to the in-phase (I) and the quadrature (Q) port of the modulators. This way, 80 Gb/s QPSK channels are obtained. The bit rate R_s is then further doubled up to 160 Gb/s per channel, by emulating polarization multiplexing through a $50/50$ beam splitter, an optical delay, and a polarization beam combiner (PBC). Thus, in this experiment, the bit rate R_s of each sub-carrier is fixed. Electrical 9^{th}-order 10 GHz low pass filter are used in order to limit the sub-carriers bandwidth and allowing a sub-carriers spacing of 20 GHz. This way a spectral occupation lower than the Nyquist bandwidth is obtained. A simple beam combiner is used as multiplexer for the odd and the even channels. A recirculating loop structure is used in order to emulate the signal transmission along different network nodes. The recirculating loop is composed by a Finisar SSS and two 40 km-long standard single mode fiber spool each one followed by an EDFA. A gain equalized filter (GEF) is used in order to balance the distortions due to the amplifier profile and a polarization scrambler (POL-S) is included in the loop emulating random signal polarization variation. The Finisar SSS emulates intermediate nodes. It is assumed *broadcast&select* node architecture [10], so traversing a node implies a single filter stage as in each loop. With such a re-circulating loop configuration, filtering effects are emphasized since a filter is traversed after just 80 km, while a link in a backbone is composed by several 8-km spans. Coherent detection as in Sec. 2 is applied with offline processing.

B. Selection of code, number of carriers and frequency slot during provisioning

The testbed described in the previous sub-section has been used to provide indications on the transmission parameters required by TFP to guarantee error-free transmission at varying the number of traversed loops. Fig. 3 reports the frequency slot width as a function of the traversed filters (or loops) when error free operation (verified for all the sub-carriers after decoding) is experienced. Some of the employed coding guaranteeing error free are reported. In these measurements, a constant information rate of 1 Tb/s is maintained considering a variable number of sub-carriers N which depends on the selected code R_C. For example, with a code rate $R_C = 8/9$, 7 sub-carriers are required to fulfill the requested 1 Tb/s information rate. With such a code, it is possible to traverse a maximum number of nodes equal to 4 with an assigned frequency slot of 150 GHz ($m = 12$), resulting in a spectral efficiency (SE) of 6.6 b/s/Hz. One more node could be traversed by increasing the redundancy, while measurements show that it is possible to simply increase the assigned spectrum up to 162.5 GHz ($m = 13$) without R_C. This is due to the fact that the detrimental filtering effects caused by the additional node hop can be overcome by enlarge the filters by only 12.5 GHz. This way no redundancy increase is required, as well as an increase of N and laser can be saved. Instead, if it is requested to traverse a higher number of nodes, it is necessary to increase the redundancy by selecting a more robust code with $R_C = 4/5$. This results in the increase of the number of sub-carriers $N = 8$, and consequently on the assigned spectrum ($175\ GHz, m = 14$), in order to maintain the super-channel capacity of 1 Tb/s (spectral efficiency of 5.7 b/s/Hz) with error-free operation. Thus, Fig. 3 shows an empirical relation between code rate, number of carriers to satisfy the information rate, physical impairments, and the frequency slot width.

C. Monitoring and code adaptation

As previously stated, during lightpath operation, a network element degradation may occur affecting the traversed signals. In this case, the code used for the lightpath can be adapted to provide more robustness against the network element degradation. In this paper, we demonstrate hitless code adaptation upon signal degradation. Such technique is based on the monitoring of the variance of the received samples, which is related to the OSNR (e.g., the larger the OSNR the lower the variance). Thanks to DSP, the variance is monitored at the coherent receiver on an active super-channel, revealing information on the OSNR. First, Fig. 4 and Fig. 5 show the relation between the variance of the acquired samples and the OSNR. Such relation has been obtained through measurements in the testbed of Fig. 2. Fig. 4 shows the OSNR range of use where the applied code with rate $R_C = 5/6$ can successfully operate ("Working" area), i.e. error free after decoding, or not ("Not working" area). Fig. 5 shows the same for a more robust code with a rate $R_C = 4/5$. Note that the variance does not depend on the applied R_C. The variance decreases with the OSNR increase. For each code, an OSNR threshold is identified at a certain margin (i.e. 1dB) from the minimum OSNR required for error free operations, thus defining the ”Margin” area. Monitoring of variances then reveals any OSNR degradation and indicates whether the working-limit condition is approaching for the code in use. Thus, while the variance is within the working condition for the considered code, no alarm is generated, but, in case of degradations, variance may increase reaching the ”Margin” area. In this case, a more robust code may be preferred. Note that, such monitoring system is able to predict OSNR degradation in advance, before reaching the ”Not working” limit conditions. If the OSNR degradation exceeds the threshold and remains within the ”Margin” area (e.g., 0.08 for 5/6 coding), no post-forward-error-correction bit error rate (post-FEC BER) degradation is experienced, but a warning alarm is locally triggered to switch, without loss of data, to a more robust code before post-FEC errors occur.

Hitless code adaptation is demonstrated as follows. First, performance degradation is introduced by adding amplified spontaneous emission (ASE) noise at the receiver. The increase of the variance is detected before the level of BER overtakes the threshold of acceptability. An alarm is generated when the variance falls within the ”Margin” area of the used code, i.e. $R_C = 5/6$. Thus, a more robust code is set without incurring in data loss because of signal degradation. In particular, code is changed to $R_C = 4/5$. Such experiment has been done considering data block of 64800 bit, plus a preamble of 448 bit including a 3-bit field. Such field is used by the source node to specify the coding applied to the subsequent data block. A sequence of three blocks is generated, each characterized by a different coding (in the first block a pre-defined coding is applied). The receiver processed and detected each data block by utilizing the coding specified in the previous data block, successfully demonstrating hitless code-adaptation and without performing complex and time-consuming re-synchronization procedures (e.g., as in the case of modulation format adaptation). Fig. 6 shows that adaptation is concluded within 2.8 ns.

IV. Conclusion

Flexibility required by lightpath provisioning in EONs was successfully demonstrated on a Terabits transmission. Experimental results showed very high spectral efficiency (6.6 b/s/Hz with PM-QPSK), effectively achieved while coping with physical layer degradations, including filtering effects. Error-free transmission is guaranteed by jointly assigning the code, the number of carriers, and the frequency slot width (i.e., the bandwidth to be switched). The paper also demonstrated how to adapt code rate during working conditions when a signal degradation occurs. Hitless code adaptation is demonstrated via software without incurring in super-channel re-routing.

Acknowledgment

This work was supported by the ORCHESTRA project.

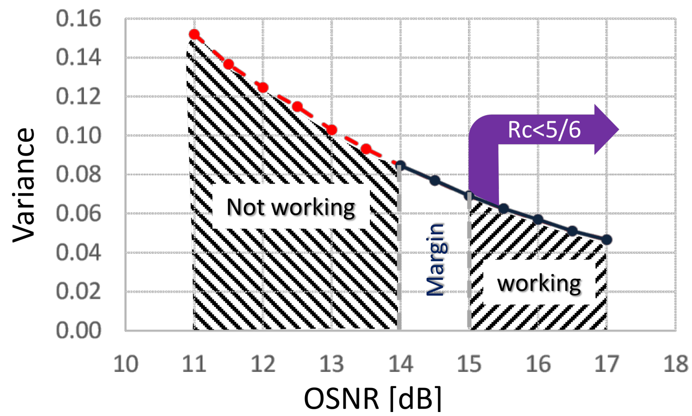

Fig. 4. Variance of the acquired samples as function of the OSNR. For code rate $R_c = 5/6$. The OSNR range of use where the applied code can successfully operate is reported (working area). The OSNR warning threshold is set opportunely at a certain margin from working limit condition. Then, the corresponding value of variance is established as threshold for monitoring operation.

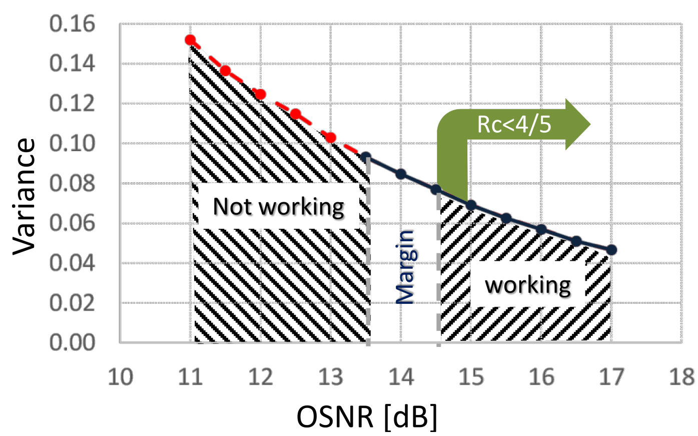

Fig. 5. Variance of the acquired samples as function of the OSNR. For code rate $R_c = 4/5$.

References

[1] M. Jinno, B. Kozicki, H. Takara, A. Watanabe, Y. Sone, T. Tanaka, and A. Hirano, “Distance-adaptive spectrum resource allocation in spectrum-sliced elastic optical path network,” *Communications Magazine, IEEE*, vol. 48, no. 8, pp. 138 –145, august 2010.

[2] K. Christodoulopoulos, I. Tomkos, and E. Varvarigos, “Elastic bandwidth allocation in flexible OFDM-based optical networks,” *Lightwave Technology, Journal of*, vol. 29, no. 9, pp. 1354 –1366, may 2011.

[3] N. Sambo, P. Castoldi, F. Cugini, G. Bottari, and P. Iovanna, “Toward high-rate and flexible optical networks,” *Communications Magazine, IEEE*, vol. 50, no. 5, pp. 66 –72, may 2012.

[4] J. Fabrega, M. Svaluto Moreolo, F. Vflchez, B. Rofoee, Y. Ou, N. Amaya, G. Zervas, D. Simeonidou, Y. Yoshida, and K. Kitayama, “Experimental demonstration of elastic optical networking utilizing time-sliceable bitrate variable OFDM transceiver,” in *Optical Fiber Communications Conference and Exhibition (OFC), 2014*, March 2014, pp. 1–3.

[5] G. Bosco, V. Curri, A. Carena, P. Poggiolini, and F. Forghieri, “On the performance of nyquist-WDM terabit superchannels based on PM-BPSK, PM-QPSK, PM-8QAM or PM-16QAM subcarriers,” *JLT*, 2011.

[6] A. Nespola, S. Straullu, G. Bosco, A. Carena, Y. Jiang, P. Poggiolini, F. Forghieri, Y. Yamamoto, M. Hirano, T. Sasaki, J. Bauwelinck, and K. Verheyen, “1306-km 20x124.8-gb/s PM-64QAM transmission over

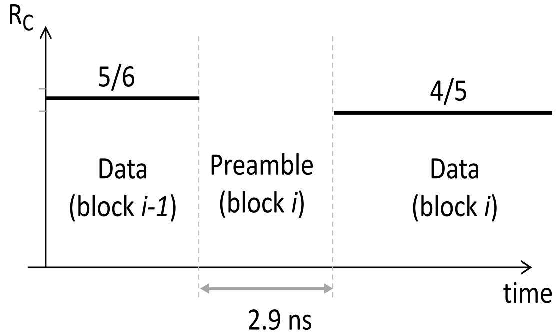

Fig. 6. Change of code and spectral efficiency.

PSCF with net SEDP 11,300 (bkm)/s/Hz using 1.15 samp/symb DAC," in *Proc. of ECOC*, 2013.

[7] D. Rafique, A. Napoli, S. Calabro, and B. Spinnler, "Digital preemphasis in optical communication systems: On the DAC requirements for terabit transmission applications," *JLT*, 2014.

[8] L. Potì, G. Meloni, G. Berrettini, F. Fresi, M. Secondini, T. Foggi, G. Colavolpe, E. Forestieri, A. D'Errico, F. Cavaliere, R. Sabella, and G. Prati, "Casting 1 Tb/s DP-QPSK communication into 200 GHz bandwidth," in *Proc. of ECOC 2012*, Sep. 2012.

[9] N. Sambo, G. Meloni, F. Paolucci, F. Cugini, M. Secondini, F. Fresi, L. Poti, and P. Castoldi, "Programmable transponder, code and differentiated filter configuration in elastic optical networks," *JLT*, 2014.

[10] N. Sambo, A. D'Errico, C. Porzi, V. Vercesi, M. Imran, F. Cugini, A. Bogoni, L. Potì, and P. Castoldi, "Sliceable transponder architecture including multiwavelength source," *JOCN*, 2014.

[11] S. Poole, S. Frisken, M. Roelens, and C. Cameron, "Bandwidth-flexible ROADMs as network elements," in *Proc. of OFC/NFOEC 2011*, 2011.

[12] L. Bahl, J. Cocke, F. Jelinek, and J. Raviv, "Optimal decoding of linear codes for minimizing symbol error rate," *Information Theory, IEEE Transactions on*, 1974.

[13] J. Hagenauer, "The turbo principle: Tutorial introduction and state of the art," in *Proc. International Symposium on Turbo Codes and Related Topics*, 1997.

[14] "Draft revised G.694.1 version 1.3," Unpublished ITU-T Study Group 15, Question 6.

[15] F. Cugini, F. Paolucci, F. Fresi, G. Meloni, G. Berrettini, N. Sambo, A. Giorgetti, T. Foggi, L. Poti, and P. Castoldi, "Benefits of active stateful PCE for flexgrid networks," in *Proc. of OFC*, 2014.

978-3-9018-8272-2/15 ©2015 IFIP